DIFFUSION OF ^{133}Xe THROUGH FROG SKINS, TOAD BLADDERS, AND WATER BOUNDARY LAYERS

GERALD L. POLLACK, *Department of Physics, Michigan State University, East Lansing, Michigan 48824 U.S.A.*

ABSTRACT We have measured the total permeability coefficients P as a function of stirring frequency ω for ^{133}Xe through frog skins and toad bladders. The permeability coefficients for the frog skins and toad bladders proper are, respectively, $P_m = (3.9 \pm 0.8) \times 10^{-4}$ cm/s and $(7.4 \pm 4.2) \times 10^{-4}$ cm/s. "Unstirred" water layer thickness δ is determined concurrently, from the frequency dependence of $P(\omega)$; the result for frog skin is $\delta = (0.060 \pm 0.016)/\sqrt{\omega(\text{rad/s})}$ cm. The stirring frequency range is from $\omega = 7.5$ rad/s (72 rpm) to 55 rad/s (530 rpm). The results support the conclusions that the principal barrier to Xe diffusion in these epithelia is inter- and intracellular water, and that the diffusion is passive and rapid. The experimental method may be straightforwardly adapted to the measurement of diffusion or counterdiffusion of any gamma-radioactive soluble or partly soluble solute through any flat membrane or through a solvent. We estimate the amount of total body-absorbed radioactivity due to environmental ^{133}Xe to be 50 fCi for an ambient concentration of 2.6 pCi/m^3 of air.

INTRODUCTION

The rare gases helium, neon, argon, krypton, and xenon are the most inert of the elements. For these elements the atomic structure, the forces between the atoms and even some of their solid state properties can be understood from quantum mechanical first principles (1, 2). Although their electron shells are complete and their chemistry relatively simple, yet these substances interact with biological systems in characteristic and interesting ways. In particular Ar and Kr, under pressure, produce narcotic or anesthetic effects in mice (3); there have been observations of cardiovascular effects of He (4) in dogs at ordinary pressures; He under high pressure, in deep sea diving, is associated with the high pressure nervous syndrome in humans, and, most interestingly, Xe is a general anesthetic for humans at 0.8 atm partial pressure (5–7).

This complex of properties means that these substances are potentially very useful as probes of living systems. They may perhaps serve as the "hydrogen atom" of biologically active chemicals. The kinds of fundamental biological questions that may be approached with these elements are: How can these atoms be used as inert probes of biological structure and interactions? What is the mechanism by which these elements cause anesthetic and narcotic effects, and can this tell us something about the

mechanism of general anesthesia? How and at what rate are these atoms transported into the body and through epithelial tissues and plasma membranes?

This paper is addressed principally to the last of these questions. We describe a measurement of the permeability coefficient P, defined as the (molar flux)/ (concentration difference), for ^{133}Xe diffusing through two epithelial tissues, viz., frog (*Rana pipiens*) abdominal skin and toad (*Bufo marinus*) urinary bladder. This work is a part of the general problem of mass transport across cell membranes and in particular across epithelia. A recent, excellent review in this field has been written by Andreoli and Schafer (8).

Studies of diffusion of rare gas atoms also have several practical applications. For example: (*a*) The radionuclide ^{133}Xe is used diagnostically in nuclear medicine; (*b*) An understanding of the narcotic effects and distribution of inert gases at high pressures is important for breathing mixtures in deep sea diving (9); and (*c*) Radioactive rare-gas isotopes ^{133}Xe and ^{85}Kr are important emissions from nuclear reactors (10–12) and must be considered in safety measures.

METHODS

The experiment consists essentially of measuring the rate at which ^{133}Xe, dissolved in amphibian Ringer's solution (NaCl, 128 mM; KCl, 5.6 mM; $NaHCO_3$, 2.4 mM; and $CaCl_2$, 2.2 mM; average pH = 8.1 ± 0.2), diffuses from one vessel to another through a membrane of frog skin or toad bladder that covers a communicating hole between the vessels. Fig. 1 shows the apparatus used. Both vessels are mainly stainless steel; they have inner diameters of 6.67 cm and are about 3.8 cm high, so that each has a volume of about 100 ml. Caps, which close the vessels on top, and bottoms of the vessels are of Lucite for visibility. The vessels contact each other at a flat surface thinned to provide a minimum-length neck and hence stirring right up to the membrane-water interface. The hole that the membrane covers has approximate diameter 2.0 cm for frog skins and 1.0 cm for toad bladders; the hole areas are, respectively, $A = \pi$ and $\pi/4$ cm^2. There is a miniature calomel electrode, not shown, in each vessel, used to continuously measure the transmembrane potential during the run. The electrodes are at the far ends of the vessels.

One important goal of this experiment is to provide as far as possible optimal stirring. This is important since the total diffusion barrier for Xe diffusion is not only the membrane itself but also an "unstirred" water layer on each side of thickness δ (13). The experiment is designed so that δ will be small and will vary with the stirring frequency ω (rad/s) in a tractable way. We shall show below that hydrodynamic and dimensional arguments suggest that $\delta(\omega) \propto \omega^{-1/2}$. We ultimately measure the permeability coefficient as a function of ω to get $P(\omega)$.

For good stirring it is important that the nondimensional parameter $r_0/(r_v - r_0)$, where r_0 is the stirrer radius (2.5 cm), and r_v is the distance from the center of the vessel to the center of the membrane, be large. For our case, for frog skins, this parameter is 8/3, close to the largest feasible value here. The idea is that the fluid's velocity when stirred is zero at the membrane surface and ωr_0 at the end of the stirrer so that $r_0/(r_v - r_0)$ is proportional to the average velocity gradient. Besides thinning the walls at the contact surface, the steel vessels were gradually beveled out around the hole in the flow direction; this helps lead the flow lines up to the membrane-water interface.

A second important aspect of the experiment is to minimize edge damage of the membranes (14–17) and its effects. Several precautions were taken for this. The membrane was held in

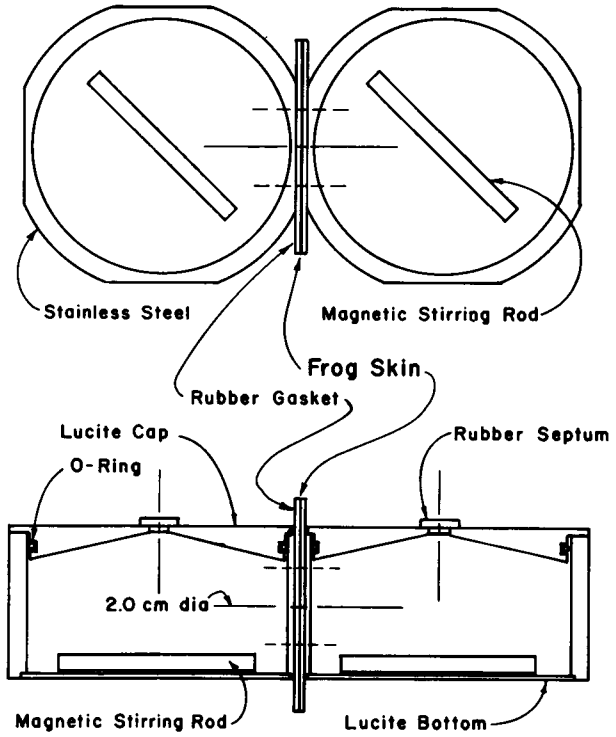

FIGURE 1 Schematic diagram of apparatus for measurement of ^{133}Xe diffusion through frog skins and toad bladders.

place between two thin rubber gaskets; for frog skins these were each 0.6 mm thick. Since the contact surfaces are flat, the area of membrane outside the hole, over which the contact force is distributed, is large (0.8 – 2.2 in^2). To further minimize the necessary contact force, the gaskets were covered with a thin layer of Dow-Corning silicone lubricant (Dow Corning Corp., Midland, Mich.). The vessels were held together with a force of 7.7 lbs by light springs with adjustable tension. This was determined to be close to the minimum force necessary to keep the vessels sealed together during the experiment. Thus the gauge pressure on the membrane outside the hole was only 4–10 lbs/in^2. This is the same pressure that the membrane would experience if the frog or toad were under 7–20 ft of water. Another parameter that keeps edge damage small is a small ratio of edge length (E) to surface area (S). For these experiments E/S = 2 (frog skins) and E/S = 4 cm^{-1} (toad bladders). At these values of E/S, Dobson and Kidder (14) observed that a frog skin generated about 89% and 84% of its full potential difference, respectively.

The frogs were wild-caught *Rana pipiens* (obtained from the University of Michigan Amphibian Facility) and the toads were large *Bufo marinus* (obtained from National Reagents, Bridgeport, Conn.). Both frogs and toads were kept well watered and were fed live crickets. The frog skins and toad bladders were dissected from freshly killed animals and mounted immediately in the experimental apparatus. In each case these membranes were inspected before and after the experiment for imperfections or damage. After each experiment the membranes were tested for watertightness; they were invariably watertight. For the groups of animals used in the present experiment, the transmembrane potential was typically 30 mV for frog

skins and 12 mV for toad bladders. During the experiment the membranes were stretched flat, whereas in nature the toad bladder is bilobed with each lobe saclike. In each case the center of the flat membrane corresponded approximately to the bottom of the sac.

It was also, of course, important in this experiment to keep the Xe in solution. The role of the O-rings around the cap and of O-rings around the electrodes was to minimize leakage of Xe and of water out of the vessel. The rubber septa at the top of the vessels, shown on Fig. 1, were held down with annular Lucite plates and screws. They allowed the vessels to be totally filled with solution initially and to be maintained full throughout the experiment. These measures also served to minimize vapor bubbles in the vessels. That was important since the water/gas Bunsen solubility for Xe is 1/8 at 22–25°C (5). This means that Xe will concentrate in vapor bubbles and give spurious concentration data. Because of this, the Ringer's solution could not be oxygenated in this experiment by bubbling oxygen through it. This may in part account for the low transmembrane potentials observed.

Xenon-133 decays to ^{133}Cs with a half-life of 5.27 days by emitting a beta ray and then an 81 keV gamma ray (18). Beta rays are very rapidly attenuated in water, but the intensity of the gamma rays, whose attenuation coefficient in water is 0.18 cm^{-1} (19), may conveniently be measured.

Both vessels were filled with Ringer's solution and a charge of about 5–10 μCi of ^{133}Xe in saline solution (Diagnostic Isotopes, Inc., Upper Saddle River, N.J.) was put into one of the vessels. Two NaI(Tl) crystals attached to photomultipliers served as gamma ray detectors, one over each vessel. These detectors were protected by lead shields of a suitable geometry so that: (*a*) Each detector was shielded from background radiation with cylindrical lead shields, 5 mm thick and 17 cm long, around each of the detectors. These shields were provided with cutouts for the electrode leads. (*b*) The detector over vessel 1 saw essentially no radiation from vessel 2 and vice versa. To achieve this condition, the detectors were recessed into the cylindrical shields and a table-shaped Pb shield was symmetrically positioned over the region of juncture of the two vessels. The tabletop was of 1 cm thick Pb so that radiation from vessel 1 was attenuated in intensity by a factor of 10^6 at detector 2, and vice versa. Finally, the detector and shield geometry was also arranged so that the membrane and stirrers were always in view. The stirring frequency is then measured with a stroboscope, twice in each vessel for each frequency.

The detectors each read into an amplifier and a single-channel analyzer set around the 81 keV radiation peak. The single-channel analyzers were both controlled by a common timer. Thus the detector over vessel 1 measured gamma radiation emitted by ^{133}Xe in vessel 1, in some fixed time interval, here usually 8 min, and the detector over vessel 2 measured the analogous quantity for vessel 2. We call N_1 and N_2 the number of ^{133}Xe atoms in vessels 1 and 2. Since the respective observed gamma radiation intensities are proportional to these, we may denote the intensities by the same symbol for convenience.

THEORY

Fick's equations for this system are:

$$dN_1(t)/dt = -PA[c_1(t) - c_2(t)] - \lambda N_1(t) \text{ and} \qquad (1a)$$

$$dN_2(t)/dt = -PA[c_2(t) - c_1(t)] - \lambda N_2(t), \qquad (1b)$$

in which P is the permeability coefficient, A is the area of the membrane available for diffusion, $c_{1,2}(t) = N_{1,2}(t)/V_{1,2}$ are the respective concentrations of ^{133}Xe in vessels 1 and 2 with $V_{1,2}$ the corresponding volumes, and, finally, $\lambda = 0.9134 \times 10^{-4}$ min^{-1} is the decay constant. We have written Eqs. 1*a* and *b* for the case that the

diffusion is symmetric and that there are no driving terms, i.e. the diffusion is passive. We shall use our results to test these assumptions.

If we add Eqs. 1*a* and *b* and then integrate, we obtain the condition for conservation of ^{133}Xe:

$$N_1(t) + N_2(t) = N_0 e^{-\lambda t}, \tag{2}$$

where $N_0 = N_1(0) + N_2(0)$ is the total initial amount of ^{133}Xe present. We tested the data of each run for conservation of Xe by Eq. 2 and this showed that on the average Xe was conserved to within 1.2%, with the worst case corresponding to loss of only 4% of the total Xe after 7 hr.

The solutions for $N_1(t)$ and $N_2(t)$ may be obtained straightforwardly by expressing Eqs. 1*a* and *b* in terms of $N_1(t)$ and $N_2(t)$, substituting from Eq. 2 to eliminate $N_2(t)$ and $N_1(t)$, and integrating the resultant first-order differential equations.

The exact solution for $N_2(t)$ satisfies:

$$N_2(t)e^{\lambda t} = [N_2(0) - N_0 V_e/V_1]\exp - (PAt/V_e) + N_0 V_e/V_1, \tag{3}$$

where $V_e = V_1 V_2/(V_1 + V_2)$ is an effective volume and we have written the decay

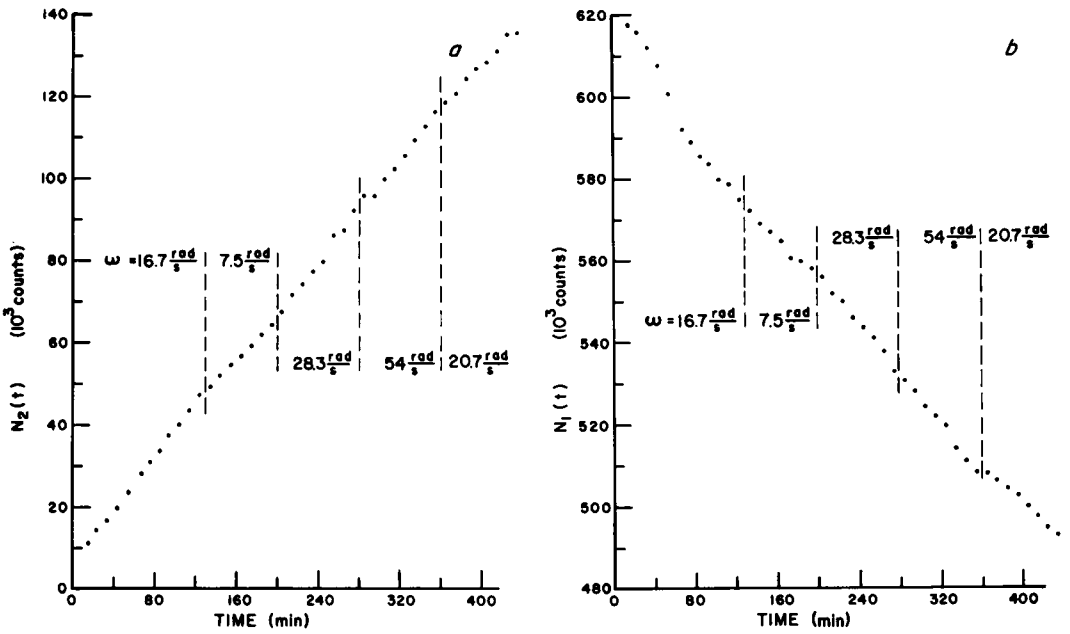

FIGURE 2 Points represent data points for one run measuring P as a function of ω for ^{133}Xe diffusing through a frog skin at mean temperature 25°C. The ordinates $N_2(t)$ and $N_1(t)$ are the numbers of counts, for a timing interval of 8 min, corrected for background, recorded on two single-channel analyzers connected to gamma-ray detectors placed over vessel 2 and vessel 1. From the data of *a* and *b*, the total permeability coefficient $P(\omega)$ is determined at each of the five values of stirring frequency, which range from $\omega = 7.5$ rad/s ($f = 72$ rpm) to 54 rad/s (516 rpm). These values are listed in Table I under frog 5.

factor $e^{\lambda t}$ on the left for convenience. The solution for $N_1(t)$ may be obtained from Eq. 3 by interchange of the indices 1 and 2 since Eq. 1*a* and 1*b* are interconvertible by this substitution. For sufficiently short time intervals, Eq. 3 may be replaced to good approximation by its linear expansion in (PAt/V_e):

$$N_2(t)e^{\lambda t} = N_2(0) - (PA/V_e)[N_2(0) - N_0V_e/V_1]t. \quad (4)$$

In using Eq. 4 we are neglecting terms of order $\frac{1}{2}(PAt/V_e)^2$ compared to (PAt/V_e). This is a contribution of a few percent to the calculated values of $P(\omega)$; the time intervals we used were too short for such parabolic dependence in $N_2(t)e^{\lambda t}$ versus t to be detectable in the data.

Our procedure then was to measure $N_1(t)$ and $N_2(t)$ simultaneously at a fixed stirring frequency ω for about 70–100 min. This, with Eq. 4, determines P at that ω. The stirring frequency was then changed to another ω and the procedure repeated. In this manner $P(\omega)$ was determined for the frog skin or toad bladder.

Figs. 2 a and b show data for $N_2(t)$ and $N_1(t)$, respectively, for a single frog skin. The frequencies at which P was measured on this frog skin are ω = 7.5 rad/s (f = 72 rpm), 16.7 rad/s (159 rpm), 20.7 rad/s (198 rpm), 28.3 rad/s (270 rpm), and 54 rad/s (516 rpm). For the time interval corresponding to each ω, the data for $N_1(t)$ and $N_2(t)$ must be converted to a common basis, to take account of the unequal sensitivities in the photomultiplier tubes, unavoidable in practice. For the present apparatus, measurement showed that at the same intensity N_2/N_1 = (1.21 ± 0.06), the necessary correction factor. For each such time interval the best linear regression fit to $N_2(t)e^{\lambda t}$ versus t is found. As may be seen from Eq. 4, the value of P for that ω may be determined from the slope of the straight line.

RESULTS

Table I displays the values of $P(\omega)$ determined in these experiments. Data are shown for experiments on five consecutive frog skins and for the four best toad bladder experiments after the experimental procedures were developed and tested. For the frog skins the experiments and their interpretation are rather more straightforward than for toad bladders. The basic difference is that frog skin (20, 21) is comparatively thicker (measured here in a calibrated dissecting microscope as 500 μm) and less easily stretched than toad bladder (22), which is thinner (100 μm) and very distensible. Thus at the higher stirring frequencies toad bladders flutter and sometimes billow. This has the effects of increasing the area available for diffusion, breaking up unstirred water layers, and stretching and thinning the membrane. Since these effects cannot be quantitatively corrected for with reliability, the data for toad bladders couldn't be treated as simply as data for frog skins. Frog skins stand up to all the ω's used here quite well. This means that for each frog skin the data on $P(\omega)$ may be considered an independent, self-consistent determination of the diffusion constant for the skin itself, as well as of the "unstirred" water layer thickness.

The values of $P(\omega)$ determined here are for diffusion for ^{133}Xe through the entire

TABLE I

DIFFUSION RATES AND STIRRING FREQUENCIES FOR FROG SKINS AND TOAD BLADDERS

Run	ω	P	P_m	δ
	rad/s	*μm/s*	*μm/s*	*cm*
Frogs	8.4	1.94	4.32	$0.056/\sqrt{\omega}$
1 (outside → inside, 24°C)	16.5	2.12		
	19.5	2.18		
	30	2.48		
	53	3.10		
2 (outside → inside, 23°C)	9.1	1.70	4.38	$0.066/\sqrt{\omega}$
	17	1.89		
	19	2.31		
	31	2.18		
	48	2.71		
3 (inside → outside, 25°C)	7.6	1.49	2.87	$0.054/\sqrt{\omega}$
	18.7	1.97		
	21.3	1.64		
	32	2.03		
	55	2.15		
4 (inside → outside, 23°C)	8.8	1.32	3.42	$0.085/\sqrt{\omega}$
	16.9	1.45		
	17.3	1.85		
	27	1.44		
	41	2.34		
5 (inside → outside, 25°C)	7.5	2.19	4.73	$0.041/\sqrt{\omega}$
	16.7	2.43		
	20.7	2.91		
	28.3	3.15		
	54	3.17		
Mean			3.94 ± 0.77	$(0.060 \pm 0.016)/\sqrt{\omega}$
Toads				
2 (mucosal → serosal, 25°C)	9.5	2.49	5.56	$0.046/\sqrt{\omega}$
	9.9	2.23		
	17.6	2.73		
	17.7	2.76		
	29	3.15		
3 (serosal → mucosal, 23°C)	9.1	4.44	7.14	$0.019/\sqrt{\omega}$
	10.1	3.92		
	18.2	4.64		
	20.1	4.69		
	29	5.02		
	52	5.62		
5 (serosal → mucosal, 27°C)	11.5	1.90	3.65	$\delta = 0.033^*/\sqrt{\omega}$
	12.3	2.17		
	19.6	2.52		
	22.9	2.92		
	30.6	3.30		
6 (mucosal → serosal, 30°C)	12.5	4.20	13.4	$\delta = 0.033^*/\sqrt{\omega}$
	13.9	4.57		
	21.5	5.28		
Mean			7.4 ± 4.2	

*Value obtained from data on toads 2 and 3 as described in text.

diffusional barrier between the vessels. This barrier consists of the membrane itself (frog skin or toad bladder) plus an "unstirred" water layer of thickness $\delta(\omega)$ at the membrane-water boundary at each side of the membrane (13). If we call P_m the permeability coefficient for ^{133}Xe through the frog skin or toad bladder proper, then the connection between the observed $P(\omega)$ and P_m is:

$$1/P = (1/P_m) + (2\delta/D_w), \tag{5}$$

where D_w is the diffusion coefficient, defined as the (molar flux)/(concentration gradient), of ^{133}Xe through water, whose value has been measured by Unsworth and Gillespie (23) as 1.2×10^{-5} cm^2/s.

The physical origin of the boundary layer is that the velocity of the fluid is zero at the membrane and increases in the region of the interface, ultimately reaching the stirring velocity ωr_0 at the stirrer tip. The thickness $\delta(\omega)$ may be defined approximately as that layer significantly depleted of ^{133}Xe by diffusion across the membrane but not sufficiently replenished by the stirred in Xe and by indiffusion of Xe through the water. The definition can only be approximate since the flow parameters are continuous.

This boundary layer occurs in hydrodynamics, where it is shown (24) that when a fluid flows with large Reynolds' number R past a body, there is a thin boundary layer, called the laminar boundary layer, in which the main velocity gradient takes place. Outside this layer the velocity rapidly approaches the flow velocity of the bulk fluid and stirring is rapid. We associate the hydrodynamic laminar boundary layer with the "unstirred" water layer of this experiment. An exact calculation of $\delta(\omega)$ requires solving the Navier-Stokes equations for our geometry and finding the velocity profile at the membrane. This is difficult for any three-dimensional configuration.

We may obtain a suggestion for the dependence of δ on ω for our experiment from the two-dimensional result: $\delta \propto L/\sqrt{R}$. In this expression L is a characteristic dimension of the body past which flow takes place, and $R = \rho u L/\eta$, where ρ and η are the fluid density and viscosity, respectively, and u is a characteristic flow velocity (24). In our experiment the only variable is u, which may be taken proportional to ω, thus $\delta \propto \omega^{-1/2}$. Support for the idea that this same dependence of δ on ω holds in three dimensions comes from a dimensional analysis argument. In addition, we have made a model calculation for the present experiment which assumes that diffusion of ^{133}Xe into the boundary layer from the bulk fluid is small compared to the stirred in ^{133}Xe and the result was $\delta \simeq \sqrt{20 P(\omega) A (r_v - r_0)/\Delta r_0 \omega}$, where Δ is the diameter of the hole and the other symbols have been previously defined. Since $P(\omega)$ is a slowly varying function we may neglect, to first approximation, its ω-dependence compared to the ω in the denominator. For these reasons we shall assume that $\delta(\omega)$ is proportional to $\omega^{-1/2}$.

With this assumption, the expected ω dependence of P may be written from Eq. 5 as:

$$1/P(\omega) = a + (b/\sqrt{\omega}). \tag{6}$$

Thus, if we plot the data in the form $1/P$ (ordinate) versus $1/\sqrt{\omega}$ (abscissa) and find

the best linear regression fit to the data, P_m may be determined from the y-intercept a as: $P_m = a^{-1}$, and δ may be determined from the slope b as: $\delta(\omega) = bD_w/2\sqrt{\omega}$.

Fig. 3 is a plot, for the run of Fig. 2 *a* and *b*, of the data in this form, including the best fitting straight line. For that frog skin $a = 2116$ s/cm, and $b = 6812$ rad$^{1/2}$ s$^{1/2}$ cm^{-1} so that $P_m = 4.73 \times 10^{-4}$ cm/s and $\delta = 0.041/\sqrt{\omega}$ cm. Table I shows the values of P_m and $\delta(\omega)$ obtained for all the frog skins and toad bladders. The mean values are: $\bar{P}_m$ (frog skin) = $(3.94 \pm 0.77) \times 10^{-4}$ cm/s, $\bar{P}_m$ (toad bladder) = $(7.4 \pm 4.2) \times 10^{-4}$ cm/s, $\bar{\delta}$ (frog skin) = $(0.060 \pm 0.016)/\sqrt{\omega(\text{rad/s})}$ cm, and $\bar{\delta}$ (toad bladders 2 and 3) = $(0.033 \pm 0.019)/\sqrt{\omega(\text{rad/s})}$ cm. The average coefficient of fit for the linear regression, Eq. 6, is $r = 0.88$ for frogs 1 through 5 and $r = 0.915$ for toads 2 and 3. Unstirred layer effects are very important in determining the total diffusion barrier. Our average results for frog skin show that the contribution to the diffusion barrier from the epithelium itself exceeds that of the unstirred water layers only at $\omega \gtrsim 15.5$ rad/s ($f \gtrsim 148$ rpm). Because of the problems often associated with toad bladders at high stirring speeds, as described above, the values of P_m for

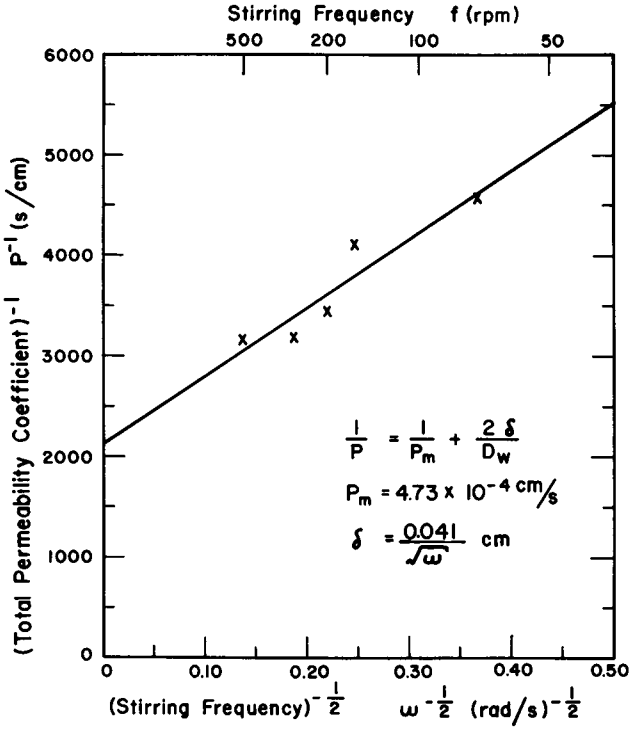

FIGURE 3 A plot of the results of the run of Fig. 2 *a* and *b* in the form $1/P$ versus $1/\sqrt{\omega}$. The x's show the individual values of $P(\omega)$. The solid line is the best linear regression fit of the form $P^{-1} = P_m^{-1} + 2\delta/D_w = a + b/\sqrt{\omega}$, where P_m is the permeability coefficient for the frog skin itself, δ is the thickness of the unstirred water layer on each side of the frog skin, D_w is the diffusion coefficient for Xe through water, a is the ordinate axis intercept and b is the slope of the straight line.

toads 5 and 6 in Table I were obtaining by assuming $\delta = 0.033/\sqrt{\omega}$, the mean value obtained for toads 2 and 3. The net result of the toad bladder distortions at high ω's is to give anomalously high values of d at those ω's. If the results are treated ignoring this, the y-intercepts are anomalously small, sometimes even negative, a physically unmeaningful result.

The method we have used here is versatile enough to be directly applied or straightforwardly adapted to many other diffusion studies. Thus it could be used to study diffusion of any gamma-ray emitting atom or molecule across any flat membrane. In our case essentially all the Xe is radioactive but one could do an experiment in which only some small fraction, large enough to be detected, of the diffusing atoms were radioactive. One could also generalize this technique to study of diffusion, or counter-diffusion, of mixtures of radioactive solutes. For this purpose the single-channel analyzers must be replaced with multichannel analyzers so that radiation from the different species may be simultaneously measured and separated by their characteristic energy emission spectra. The method can also be applied to study diffusion of radioactive ions or soluble molecules through membranes. In those cases no extra precautions need be taken to prevent escape of the solute by evaporation, as were necessary in the present experiment. Finally, the method can be used to measure the diffusion coefficient of any of these solutes through any solvent, e.g. water, alcohol, olive oil, etc. For that application the membrane must be replaced by a thin plate with suitable holes of known dimensions in it.

CONCLUSION

We may compare our mean value of $\delta(\omega)$ for frog skin, calculated from Table I as $\bar{\delta}(\omega) = (0.060 \pm 0.016)/\sqrt{\omega(\text{rad/s})}$ cm, with estimates of Dainty and House (13) of unstirred layers in frog skin. For the lowest frequency we used, 7.5 rad/s (72 rpm), our result is $\bar{\delta} = 160$–280 μm and for our highest frequency, 55 rad/s (530 rpm), our result is $\bar{\delta} = 59$–100 μm. The total unstirred layer diffusion barrier for these cases is, therefore, $2\bar{\delta} = 320$–560 and 118–220 μm, respectively. Dainty and House (13) report total unstirred layer diffusion barriers of 190–290 μm at 120 rpm and 100–170 μm at 500 rpm. The agreement between their results and our $\bar{\delta}(\omega)$ is good, especially at high frequencies.

Our data and results show that ^{133}Xe diffusion for frog skins and toad bladders follows Eqs. 2*a* and *b* and we therefore conclude that within our experimental limits the diffusion of Xe across these epithelia is the same in both directions and passive, i.e. not driven. Further support for the former conclusion comes from Table I, where we report the experiments on frog skins in which the main Xe flux is from outside to inside separately from those for which the main flux is in the other direction. Table I also reports the experiments on toad bladders in which the main flux is from mucosal (urine) to serosal (blood) side separately from those with main flux from serosal to mucosal side.

The magnitudes of the permeability coefficients as given in Table I, namely $\bar{P}_m$

(frog skins) = (3.9 ± 0.8) × 10^{-4} cm/s and $\bar{P}_m$ (toad bladders) = (7.4 ± 4.2) × 10^{-4} cm/s lead us to the further conclusion that Xe diffusion through these epithelia is fairly rapid. Thus these values may be compared with earlier measurements of Hays and Leaf (25, 26) of the permeability coefficient of toad bladder to water, solutes, and ions and with more recent measurements of Hays (27) and Hays and Franki (28) of the permeability coefficient to tritiated water (THO). Our values for $\bar{P}_m$ are larger than the earlier maximum value they report, viz. 1.58 × 10^{-4} cm/s for water molecules when the toad bladder was treated with vasopressin (25, 26). However, in the more recent work (27, 28), which takes into account unstirred layers by extrapolation to infinite stirring speeds, a value of 7.1 × 10^{-4} cm/s was obtained for the permeability coefficient of THO through intact toad bladders. From additional measurements on toad bladders from which the epithelial cells have been scraped off, it was concluded that the permeability coefficient of the epithelial cell layer alone would be considerably larger, 19 × 10^{-4} cm/s. The rapid transport of Xe through epithelia is consistent with the atom's small size and nonpolar nature.

Our observation of rapid, passive, diffusion of Xe through epithelia is in contrast to the results of a recent study of Xe accumulation in red blood cells by Dragomir et al. (29). Those workers measured the permeability coefficient of ^{133}Xe through erythrocyte membranes and obtained (1.73 ± 0.74) × 10^{-6} cm/s, a value only 1/200 of our value for frog skins. They observed, in addition, Xe accumulation into the erythrocyte so that the concentration inside exceeded the concentration outside by 20%. Among the possible theoretical consequences of their work they consider active transport of Xe itself, coupling of Xe transport into the cell with some other actively transported ion or molecule, and intracellular adsorption independent of pumping. A unified understanding of our results and their results must await further experiments on these different systems.

Unsworth and Gillespie (23) have measured the diffusion coefficient D for ^{85}Kr and ^{133}Xe on 1-mm-thick slices of biological tissues. Their results for ^{133}Xe were D = 0.68 × 10^{-5} cm^2/s for dog muscle and 0.29 × 10^{-5} cm^2/s for sheep liver tissues, at 37°C. To make these measurements, they assumed that the inert gas atoms diffused uniformly throughout the samples. Under that assumption we may calculate the permeability coefficients for these tissues as $P = D/(\text{thickness})$ = 0.68 × 10^{-4} cm/s for dog muscle and 0.29 × 10^{-4} cm/s for sheep liver tissues.

Our results enable us to discuss the diffusion barrier and the mechanism of Xe diffusion through frog skins and toad bladders. We note first that the calculated permeability coefficient through a layer of water θ cm thick is $P = D_w/\theta$ = (1.2 × 10^{-5})/θ, using the previous value of D_w (23). If we replace the frog skin and toad bladder by a layer of water equal to their approximate thicknesses, 500 μm and 100 μm, then we calculate 2.4 × 10^{-4} cm/s and 12 × 10^{-4} cm/s, respectively. The frog skin result is only 25% below the experimental lower limit for P_m shown on Table I and the toad bladder result is slightly higher than the respective experimental upper limit.

Our results are thus consistent with the conclusion that the principal barrier to diffusion of Xe through frog skins and toad bladders is the inter- and intracellular water.

These epithelia act as unstirrable layers of water equal to the membrane thickness. We picture the Xe as passively diffusing through this water. That implies that the contribution to the diffusion barrier presented to the Xe by the plasma membranes may be relatively unimportant. This result is probably generalizable for Xe diffusion through other relatively thick epithelia. It is not surprising that the diffusion barrier presented by the plasma membrane is small compared to the diffusion barrier of the cell water. These two barriers are generally in series and the resistance to diffusion of each barrier may be defined as its thickness divided by the diffusion coefficient for Xe through the material of the barrier (see for example, Eq. 5). Since the plasma membrane thickness is much less than the thickness of the cell interior, its resistance to diffusion will be relatively small, unless D in the membrane is much smaller than in the rest of the cell.

Schafer and Andreoli (30) have considered the diffusional resistance of cells to water in connection with their experiments on water transport in mammalian cortical collecting tubules. They suggest that the diffusional resistance of the epithelial cell layer might be substantially greater than that of an equivalent layer of water. Parisi and Piccinni (31) have done experiments on the movement of THO through and into toad urinary bladders and discussed the diffusional permeability of this epithelium.

For Xe diffusing through much thinner epithelial membranes, for example the alveolar membrane, the barrier presented by the plasma membrane may be more important relative to the cellular fluid barrier. However, in that case the limit to diffusion is probably set by the external unstirred layers.

Kunz and Paperiello (12) have recently measured the ambient radioactive concentration of ^{133}Xe in the air and obtained 2.6 pCi/m^3 of air, due to gaseous effiuents from nuclear reactors in the northeastern United States. Since we know that diffusion of ^{133}Xe through epithelia is rapid, it is important to estimate how much radioactivity in the form of ^{133}Xe is inside a person in equilibrium with this air. Bunsen solubilities of Xe at 37°C are 0.085 for water/gas and 1.78 for olive oil/gas (5). We take the solubility in olive oil as approximately the solubility in body lipids. Thus if we consider a 70-kg man to contain 41 kg of water and 9 kg of lipids and neglect the ^{133}Xe in the rest of his body, and if we further take the density of the body lipids to be the same as water, we obtain: total ^{133}Xe in body water = (2.6)(0.085)(0.041) pCi = 9.1 fCi; Total ^{133}Xe in body lipids = (2.6)(1.78)(0.009) pCi = 42 fCi. This gives a total body radioactivity of 50 fCi due to ambient ^{133}Xe.

It is also interesting to calculate the analogous quantity for ^{85}Kr. Krypton-85 is a long-lived (half-life 10.76 years), beta-emitting radioisotope produced, as noted earlier, in nuclear fission. Boeck (32) has recently considered a concentration level of ^{85}Kr of 3 nCi/m^3 of air, a level projected for the early part of the next century. Bunsen solubilities of Kr at 37°C are 0.0505 for water/gas and 0.443 for olive oil/gas (5). Under the same assumptions for a 70-kg man, as in the above calculation for ^{133}Xe, we calculate the total ^{85}Kr in body water as 6.2 pCi and the total ^{85}Kr in body lipids as 12.0 pCi. Thus the total body radioactivity is 18 pCi of ^{85}Kr at an ambient level of 3 nCi/m^3.

In the event of a nuclear accident, such as a core meltdown or a nuclear explosion, the ambient ^{133}Xe and ^{85}Kr levels could be large multiples of 2.6 pCi/m^3 and 3 nCi/m^3. The total amount of body radiation due to absorption by the body of each of these nuclear species would then be the same multiples of 50 fCi and 18 pCi.

I thank D. K. Christen, W. L. Frantz, J. Mountz, J. Terris, H. T. Tien, and the late R. M. Featherstone for their help. I am in particular indebted to Professor G. Bertsch for the model calculation of $P(\omega)$ and for several discussions related to this work.

This research was supported by Energy Research and Development Administration Grant AT(11-1)-1574.

Received for publication 29 December 1976 and in revised form 22 March 1977.

REFERENCES

1. POLLACK, G. L. 1964. The solid state of rare gases. *Rev. Mod. Phys.* **36**:748–791.
2. KLEIN, M. L., and J. A. VENABLES, editors. 1976. Rare Gas Solids, Volume I. Academic Press, Ltd., London, U.K.
3. MILLER, K. W., and E. B. SMITH. 1973. Intermolecular forces and the pharmacology of simple molecules. *In* A Guide to Molecular Pharmacology-Toxicology R. M. Featherstone, editor. Marcel Dekker, Inc., New York. 427–475.
4. RAYMOND, L., R. B. WEISKOPF, M. J. HALSEY, A. GOLDFEIN, E. I. EGER, II, and J. W. SEVERINGHAUS. 1972. Possible mechanism for the antiarrhythmic effect of helium in anesthetized dogs. *Science (Wash. D.C.).* **176**:1250–1252.
5. SEEMAN, P. 1972. The membrane actions of anesthetics and tranquilizers. *Pharmacol. Rev.* **24**:583–655.
6. FEATHERSTONE, R. M., and C. A. MUEHLBACHER. 1963. The current role of inert gases in the search for anesthesia mechanisms. *Pharmacol. Rev.* **15**:97–121.
7. CULLEN, S. C., and E. G. GROSS. 1951. The anesthetic properties of Xenon in animals and human beings, with additional observations on Krypton. *Science (Wash. D.C.).* **133**:580–582.
8. ANDREOLI, T. E., and J. A. SCHAFER. 1976. Mass transport across cell membranes: the effects of antidiuretic hormone on water and solute flows in epithelia. *Annu. Rev. Physiol.* **39**:451–500.
9. BENNETT, P. B., and D. H. ELLIOTT, editors. 1969. The Physiology and Medicine of Diving and Compressed Air Work. Williams and Wilkins, Baltimore, Md. especially chapters 7, 8, and 15.
10. United States Atomic Energy Commission. 1974. Reactor Safety Study, draft WASH-1400 U.S. Atomic Energy Commission, Washington, D.C.
11. United States Atomic Energy Commission. 1970. Chart of the Nuclides. U.S. Government Printing Office, Washington, D.C.
12. KUNZ, C. O., and C. J. PAPERIELLO. 1976. Xenon-133: ambient activity from nuclear power stations. *Science (Wash. D.C.).* **192**:1235–1237.
13. DAINTY, J., and C. R. HOUSE. 1966. 'Unstirred layers' in frog skin. *J. Physiol. (Lond.).* **182**:66–78.
14. DOBSON, J. G., JR., and G. W. KIDDER, III. 1968. Edge damage effects in in vitro frog skin preparations. *Am. J. Physiol.* **214**:719–724.
15. WALSER, M. 1970. Role of edge damage in sodium permeability of toad bladder and means of avoiding it. *Am. J. Physiol.* **219**:252–255.
16. HELMAN, S. I., and D. A. MILLER. 1973. Edge damage effect on electrical measurements of frog skin. *Am. J. Physiol.* **225**:972–977.
17. LEWIS, S. A., and J. M. DIAMOND. 1975. Active sodium transport by mammalian urinary bladder. *Nature (Lond.).* **253**:747–748.
18. LEDERER, C. M., J. M. HOLLANDER, and I. PERLMAN. 1968. Table of Isotopes. Sixth edition. John Wiley and Sons, Inc., New York. 280–281
19. DAVISSON, C. M. 1965. Gamma-ray attenuation coefficients. B. Attenuation of various substances. *In* Alpha-, Beta-, and Gamma-Ray Spectroscopy, Vol. 1, K. Siegbahn, editor. North-Holland Publishing Co., Inc. Amsterdam. Appendix 1. 842.
20. FARQUHAR, M. G., and G. E. PALADE. 1965. Cell junctions in amphibian skin. *J. Cell Biol.* **26**:263–291.

21. VOUTE, C. L. 1963. An electron microscopic structure of the skin of the frog (*Rana pipiens*). *J. Ultrastruct. Res.* **9**:497–510.
22. PEACHEY, L. D., and H. RASMUSSEN. 1961. Structure of the toad's urinary bladder as related to its physiology. *J. Biophys. Biochem. Cytol.* **10**:529–553.
23. UNSWORTH, J., and F. C. GILLESPIE. 1971. Diffusion coefficients of xenon and krypton in water from 0° to 80°C and in biological tissue at 37°C. *In* Diffusion Processes, Volume 2, J. N. Sherwood et al., editors. Gordon & Breach, Science Publishers, Inc., New York. 599–608.
24. LANDAU, L. D., and E. M. LIFSHITZ. 1959. Fluid Mechanics. Pergamon Press, Oxford, U.K. Chapter IV, section 39. 145–151.
25. HAYS, R. M., and A. LEAF. 1962. Studies on the movement of water through the isolated toad bladder and its modification by vasopressin. *J. Gen. Physiol.* **45**:905–919.
26. LEAF, A., and R. M. HAYS. 1962. Permeability of the isolated toad bladder to solutes and its modification by vasopressin. *J. Gen. Physiol.* **45**:921–932.
27. HAYS, R. M. 1972. The movement of water across vasopressin-sensitive epithelia. *Curr. Top. Membranes Transp.* **3**:339–366.
28. HAYS, R. M., and N. FRANKI. 1970. The role of water diffusion in the action of vasopressin. *J. Membr. Biol.* **2**:263–276.
29. DRAGOMIR, C. T., D. T. STEFĂNESCU, I. GEORGESCU, G. N. STERE, L. CIUCĂ, D. UNGUREANU, F. TUDOR, and R. CHIRVASIE. 1975. Xenon accumulation in the red blood cell. A process altered by suppressors of the membrane active transport function. *Biochim. Biophys. Acta.* **389**:530–540.
30. SCHAFER, J. A., and T. E. ANDREOLI. 1972. Cellular constraints to diffusion. The effect of antidiuretic hormone on water flows in isolated mammalian collecting tubules. *J. Clin. Invest.* **51**:1264–1278.
31. PARISI, M., and Z. F. PICCINNI. 1973. The penetration of water into the epithelium of toad urinary bladder and its modification by oxytocin. *J. Membr. Biol.* **12**:227–246.
32. BOECK, W. L. 1976. Meteorological consequences of atmospheric Krypton-85. *Science (Wash. D.C.).* **193**:195–198.